Mathematics

http://www.aimspress.com/journal/Math

AIMS Mathematics, 6(8): 8625–8641.
DOI: 10.3934/math.2021501
Received: 25 January 2021
Accepted: 27 April 2021
Published: 07 June 2021

Research article

Smooth path planning via cubic GHT-Bézier spiral curves based on shortest distance, bending energy and curvature variation energy

Samia BiBi[1], **Md Yushalify Misro**[1,*] **and Muhammad Abbas**[2,*]

[1] School of Mathematical Sciences, Universiti Sains Malaysia, Penang 11800, Malaysia
[2] Department of Mathematics, University of Sargodha, Sargodha 40100, Pakistan

* **Correspondence:** Email: yushalify@usm.my, muhammad.abbas@uos.edu.pk.

Abstract: In this article, an algorithm to obtain a smooth path (free from obstacles) that can be optimized by shortest path distance, bending energy and curvature variation energy will be presented. Previously, scholars used various tools to generate smooth path such as Clothoid, Log-Aesthetic curves (LACs), and Bézier curves. The limited number of solutions from the aforementioned curves become one of the drawback to generate smooth path planning. Therefore, providing a number of solutions that can generate smooth path planning becomes the objective of this study. In this paper to generate a smooth path, five templates of spiral transition curves having three different shape parameters with monotone curvature (either increase or decrease) by cubic GHT-Bézier curves are proposed. Moreover, few examples of path planning technique via cubic GHT-Bézier spiral curve to show the flexibility of smooth path by minimization of the shortest path (minimum arc length) **L**, bending energy **E** and curvature variation energy **V** are presented. The superiority of cubic GHT-Bézier spiral path smoothing techniques as compared to Clothoid and LACs is also demonstrated.

Keywords: cubic GHT-Bézier curve; shape parameters; spiral curves; monotone curvature; minimum arc length; bending energy; curvature variation energy
Mathematics Subject Classification: 53A04, 49Q10

1. Introduction

Continuous path planning can be defined as smooth motion from the initial location to the final goal without any hurdle. Parametric curves such as Bézier curves and B-spline curves are widely used in CAD/CAM and engineering field. The smooth path can be obtained by two techniques such as parametric representation like Bézier and non-linear representation as Clothoid. Despite Bézier or B-spline curves are widely used in CAD/CAM field, but when we obtain any smooth path by using them it gives us complicated curvature computation. So, in order to tackle this problem spiral transition curves by GHT-Bernstein basis are presented, which provides us a smooth path with simple curvature computation.

The theory of curves and surfaces can be studied in [1]. Some spiral curves are constructed by cubic Bézier curve [2], however, these spiral curves lose their degree of freedom while satisfying the monotonicity of curvature. There are also attempts to represent spiral transition curves having monotone curvature by Misro et al. [3]. They present five templates of spiral curves by cubic trigonometric Bézier curve. In [4, 5], a technique for composing a fair curve from the pair of Pythagorean hodograph quintic spiral segments is examined and presented by joining two different points. Sakai and Habib [6] and Misro et al. [7], proposed a method for joining two circles with S-shape and C-shape transition curve with two spiral segments. An obstacle avoiding smooth path with Log-Aesthetic curves based on minimal arc length is presented by Gobithaasan et al. [8]. They presented an algorithm for smooth path planning.

In [9], Li et al. proposed a method that is used to replace the polyline path by G^2 cubic spline curve to obtain a smooth path. Misro et al. [10, 11] constructed spiral transition curves by cubic and quintic trigonometric Bézier curve having two dynamic parameters. The extended analysis is conducted by determining the range of dynamic parameters. A new analytical tool for the gradual transition of clearance from zero value on straight sections to the minimum value at the center of horizontal curves is presented by Mauga [12]. In [13], special Clothoid templates by joining Clothoid to Clothoid and Clothoid to circle to the sketched alignment can be obtained by various applications of the spline. Haveman et al. [14], presented an algorithm for Clothoid interpolation that can also be used for curve fitting, curvature smoothing, and for directly editing the curvature as well. By using G^2 Hermite interpolation, Log-Aesthetic curves are developed by Miura et al. [15]. They are also used for many practical applications in the CAD/CAM field. In [16], an algorithm is presented for shape completion by Log-Aesthetic Curves (LAC) with C-shape or S-shape. BiBi et al. [17] described generalized hybrid trigonometric Bézier (GHT-Bézier) curves with its various properties. Comparison of curvature junction by classical Bézier curve and by GHT-Bézier curve is also proposed. BiBi et al. [18], also described GHT-Bernstein basis functions with GHT-Bézier curve having an extra trigonometric function involving shape parameter λ. Various symmetric revolutionary curves and symmetric rotation surfaces are also constructed by using this literature. In [19], the construction of Bézier curves and Bézier surfaces is done by Hu et al. The continuity conditions between two adjacent curves and surfaces are also presented with various modelings. The parametric and geometric continuity constraints between any two curves and surfaces are derived in [20, 21]. Chen and Ma [22], present a local piecewise geometric interpolation method for the B-spline interpolation problem with tangent directional constraints. The method is based on an unclamping technique and knot extension. The interpolation problem is made to find a cubic B-spline curve which interpolates both the positions of the points and their tangent directional vectors. Some engineering Bézier surfaces and developable Bézier surfaces are also constructed by having multiple shape parameters and by continuity constraints between two adjacent surfaces [23, 24].

In this paper by using GHT-Bézier curve five templates of spiral transition curves are constructed. These spiral curves are very helpful in designing highways and to avoid sudden accidents caused by a sharp turn. Moreover, an algorithm is presented by cubic GHT-Bézier spiral curve for smooth path planning based on minimum arc length (the Shortest Distance) **L**, Bending Energy **E** and Curvature Variation Energy **V**. These values provide us suitable path to move from any initial location to the final position. It is evident that due to various shape parameters of GHT-Bézier spiral curves, it can provide us multiple solutions of **L**, **E** and **V** as compared to Log-Aesthetic curve. So, we can obtain the shortest smooth path free from obstacles by minimization of **L**, **E** and **V**.

This paper is summarized in seven sections. In Section 2, some useful formulas and background of this literature are described. The cubic GHT-Bernstein basis functions and cubic GHT-Bézier curve with its properties such as convex hull property, symmetry, positivity and endpoint properties are described in Section 3. The construction of five templates of GHT-Bézier spiral curves are described in Section 4. In Section 5, an algorithm for the smooth path (free from obstacles) is proposed. Description of smooth path algorithm are discussed in Section 6. Moreover, some numerical examples are presented in Section 7 to ensures that a smooth obstacle avoiding path is obtained by minimization of the Shortest path, Bending Energy, and Curvature Variation Energy. Finally, a summarized conclusion is given in Section 8.

2. Background notations and analytical formulas

In cartesian coordinate system the following familiar notations are used which are also very helpful for this study. The parametric form of any vector $\vec{u}$ can be written as $\vec{u} = (\vec{u}_x, \vec{u}_y)$, while Euclidean norm of vector $\vec{u}$ can be defined as $||\vec{u}|| = \sqrt{\vec{u}_x^2 + \vec{u}_y^2}$. The cross product between two vectors can be defined as,

$$\vec{u} \times \vec{v} = \vec{u}_x \vec{v}_y - \vec{u}_y \vec{v}_x = ||\vec{a}||||\vec{b}||sin\theta,$$

where angle θ is measured in anti clockwise direction. The unit tangent vector for any curve $S(u)$ can be defined as follows,

$$T_0 = \frac{S^{'}(0)}{||S'(0)||}, \qquad T_1 = \frac{S^{'}(1)}{||S'(1)||}.$$

The curvature κ and its derivative $\kappa^{'}$ in terms of variable u is defined in Eqs (2.1) and (2.2) respectively,

$$\kappa(u) = \frac{S^{'}(u) \times S^{''}(u)}{||S'(u)||^3} = \frac{2(x(u)y^{'}(u) - x^{'}(u)y(u))}{(x^2(u) + y^2(u))^2}. \tag{2.1}$$

and

$$\kappa^{'}(u) = \frac{h(u)}{||S'(u)||^5} \tag{2.2}$$

where

$$h(u) = ||S^{'}(u)||^2 \frac{d}{du}(S^{'}(u) \times S^{''}(u)) - 3(S^{'}(u) \times S^{''}(u))(S^{'}(u).S^{''}(u)).$$

3. Cubic GHT-Bézier curve

Definition 1. *The Quadratic hybrid trigonometric Bernstein basis function interms of variable u and having shape parameters* $\alpha, \beta, \gamma \in [-1, 1]$ *can be defined as follows,*

$$\begin{cases} L_{0,2}(u) = (1 - sin(\frac{\pi}{2}u))(1 - \alpha sin(\frac{\pi}{2}u))e^{\gamma u} \\ L_{1,2}(u) = 1 - L_{0,2}(u) - L_{2,2}(u) \\ L_{2,2}(u) = (1 - cos(\frac{\pi}{2}u))(1 - \beta cos(\frac{\pi}{2}u))e^{(1-\gamma)u}. \end{cases}$$

For integer $n = 3$, $0 \leq i \leq 3$, the cubic GHT-Bernstein basis function $L_{i,3}(u)$ is recursively defined as [17],

$$L_{i,3}(u) = (1-u)L_{i,2}(u) + uL_{i-1,2}(u). \tag{3.1}$$

A cubic GHT-Bézier curve with given set of control points $\widetilde{P_i}$, where $(i = 0,1,2,3)$ and shape parameters α, β and γ is given in Eq (3.2):

$$S(u;\alpha,\beta,\gamma) = \sum_{i=0}^{3} \widetilde{P_i} L_{i,3}(u), \quad 0 \leq u \leq 1. \tag{3.2}$$

Figure 1 shows the graphical representation of cubic GHT-Bernstein basis and cubic GHT-Bézier curve with different values of shape parameters.

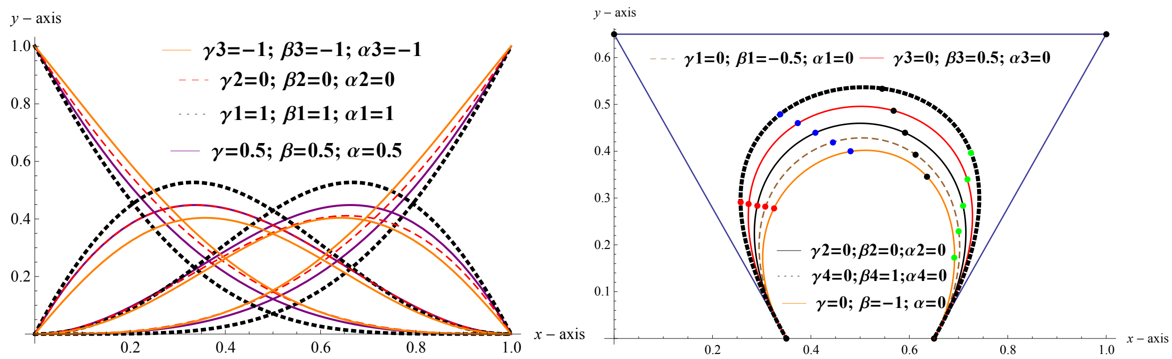

(a) Cubic GHT-Bernstein basis function

(b) Cubic GHT-Bézier Curve

Figure 1. Graphical representation of cubic GHT-Bernstein basis function and cubic GHT-Bézier curve.

Theorem 1. *Cubic GHT-Bézier curve possess various properties like convex hull property, symmetry, shape adjustable property, variation diminishing property, and endpoint interpolation property.*

Proof. The proof of the following properties like convex hull property, symmetry, shape adjustable property, variation diminishing property is as described in [17]. While the endpoint interpolation property for cubic GHT-Bézier curve is defined as follows:

$$\begin{cases} S(0) = \widetilde{P_0}, \\ S(1) = \widetilde{P_3}, \\ S'(0) = (1 + \frac{\pi}{2}(1+\alpha) - \gamma)(\widetilde{P_1} - \widetilde{P_0}), \\ S'(1) = (1 + \frac{\pi}{2}(1+\beta) - \gamma)(\widetilde{P_3} - \widetilde{P_2}), \\ S''(0) = (\pi(1+\alpha) + \frac{1}{2}\pi^2\alpha - (2+\pi)\gamma - \pi\alpha\gamma + \gamma^2)\widetilde{P_0} + (-2\pi(1+\alpha) - \frac{1}{2}\pi^2\alpha - \frac{1}{4}e^{\gamma}\pi^2(1-\beta) \\ +\gamma(4+\pi+\pi\alpha-\gamma))\widetilde{P_1} + (\pi(1+\alpha) + \frac{1}{4}e^{\gamma}\pi^2(1-\beta) - 2\gamma))\widetilde{P_2}, \\ S''(1) = (\pi + \frac{1}{4}e^{\gamma}\pi^2(1-\alpha) + \pi\beta - 2\gamma)\widetilde{P_1} + (-2\pi - \frac{1}{4}e^{\gamma}\pi^2(1-\alpha) - 2\pi\beta - \frac{\pi^2}{2}\beta + \gamma(4+\pi) \\ +\pi\beta\gamma - \gamma^2)\widetilde{P_2} + (\pi(1+\beta) + \frac{1}{2}\pi^2\beta - 2\gamma - \pi\gamma - \pi\beta\gamma + \gamma^2)\widetilde{P_3}. \end{cases} \tag{3.3}$$

□

4. Joining cubic GHT-Bézier curves to circles and lines

This section presents different cubic GHT-Bézier spiral curve segments. The five templates for cubic GHT-Bézier spiral curves are given as follows:

- Straight line to circle with cubic GHT-Bézier spiral curve.
- Circle in circle with cubic GHT-Bézier spiral curve.
- Circle to circle forming S-shape curve with two cubic GHT-Bézier spiral curves.
- Circle to circle forming C-shape curve with two cubic GHT-Bézier spiral curves.
- Line to line with cubic GHT-Bézier spiral curve.

4.1. Straight line to circle with cubic GHT-Bézier spiral curve

Theorem 2. *Consider T_0 and T_1 be the first and last unit tangent vectors and $\widetilde{P_0}, \widetilde{P_1}, \widetilde{P_2}$ and $\widetilde{P_3}$ are the control points. The cubic GHT-Bézier Spiral curve can be defined by the following control points as follows:*

$$\begin{cases} \widetilde{P_1} = \widetilde{P_0} + \frac{50r(1+\frac{\pi}{2}(1+\alpha)-\gamma)tan\theta}{108cos\theta}T_0, \\ \widetilde{P_2} = \widetilde{P_1} + \delta\frac{50r(1+\frac{\pi}{2}(1+\beta)-\gamma)tan\theta}{108cos\theta}T_0, \\ \widetilde{P_3} = \widetilde{P_2} + \frac{\frac{\pi}{2}(1+\alpha)tan\theta}{18}T_1, \end{cases} \tag{4.1}$$

where angle θ is measured in anti clockwise from T_0 to T_1 and for cubic GHT-Bézier spiral curve we have the following conditions,

$$T_0 = \frac{S^{'}(0)}{||S^{'}(0)||}, \qquad T_1 = \frac{S^{'}(1)}{||S^{'}(1)||}, \qquad \kappa(0) = 0, \qquad \kappa(1) = \frac{1}{r}, \qquad \kappa^{'}(1) = 0.$$

Proof. By using end point properties of cubic GHT-Bézier curve given in Eq (3.3) and by having $\kappa(0) = 0$, we have

$$(1 + \frac{\pi}{2}(1 + \alpha) - \gamma)||\widetilde{P_1} - \widetilde{P_0}||(\pi + \frac{1}{4}e^{\gamma}\pi^2(1 - \beta) + \pi\alpha - 2\gamma)||\widetilde{P_2} - \widetilde{P_1}||sin\theta = 0. \tag{4.2}$$

Now by using $\kappa(1) = \frac{1}{r}$ and by repeating similar steps, we have the following result,

$$||\widetilde{P_1} - \widetilde{P_0}|| = \frac{50r(1 + \frac{\pi}{2}(1 + \alpha) - \gamma)tan\theta}{108cos\theta}, \tag{4.3}$$

and for $\kappa^{'}(1) = 0$, we have

$$||\widetilde{P_3} - \widetilde{P_2}|| = \frac{10r\frac{\pi}{2}(1 + \alpha)tan\theta}{18}. \tag{4.4}$$

Let we consider

$$||\widetilde{P_2} - \widetilde{P_1}|| = \delta||\widetilde{P_1} - \widetilde{P_0}||,$$

where $\delta > 0$, so we will obtain

$$||\widetilde{P_2} - \widetilde{P_1}|| = \delta\frac{50r(1 + \frac{\pi}{2}(1 + \alpha) - \gamma)tan\theta}{108cos\theta}. \tag{4.5}$$

Hence, the control points for cubic GHT-Bézier spiral curve is defined in Eq (4.6),

$$\begin{cases} \widetilde{P_1} = \widetilde{P_0} + \frac{50r(1+\frac{\pi}{2}(1+\alpha)-\gamma)tan\theta}{108cos\theta}T_0, \\ \widetilde{P_2} = \widetilde{P_1} + \delta\frac{50r(1+\frac{\pi}{2}(1+\beta)-\gamma)tan\theta}{108cos\theta}T_0, \\ \widetilde{P_3} = \widetilde{P_2} + \frac{\frac{\pi}{2}(1+\alpha)tan\theta}{18}T_1. \end{cases} \tag{4.6}$$

□

Position: Suppose that a straight line is given on the x-axis and the center of the circle is positioned in the first quadrant. Let S be the radius of the circle and Q be the distance from x-axis to the center of the circle.

Condition: Since the shape parameters for cubic GHT-Bézier curve are $\alpha, \beta, \gamma \in [-1, 1]$. So, we choose different values of shape parameters and angle θ to obtain the solution. Figure 2(a) shows the cubic GHT-Bézier spiral curves with different shape parameters and different values of θ as mentioned.

- When $\theta = \frac{\pi}{5}$, and shape parameters are $\alpha = -1, \beta = -0.5, \gamma = -1$, the solution (path from origin to straight line) of cubic GHT-Bézier curve is obtained as $Q > S$. While the chosen values of Q and S in this case are 0.81 and 0.43 respectively. Its curvature is monotone as shown in Figure 2b (red curve).
- When $\theta = \frac{\pi}{6}$, and shape parameters are $\alpha = 0, \beta = 0, \gamma = 0$, the solution of cubic GHT-Bézier curve is again obtained as $Q > S$. The chosen values of Q and S in this case are 0.623 and 0.43 respectively. The curvature profile is given in Figure 2(b) (black curve) with monotone behavior.
- When $\theta = \frac{\pi}{10}$, and $\alpha = 0.5, \beta = 0, \gamma = -0.5$, the solution is obtained when $Q = S$, the chosen values for radius of the circle S and Q (distance from the origin to the x-axis) are equal, i.e. $S = Q = 0.43$. So, in this case curvature of cubic GHT-Bézier spiral curve also changes monotonically and graphical representation of curvature profile is given in Figure 2(b) (blue curve).

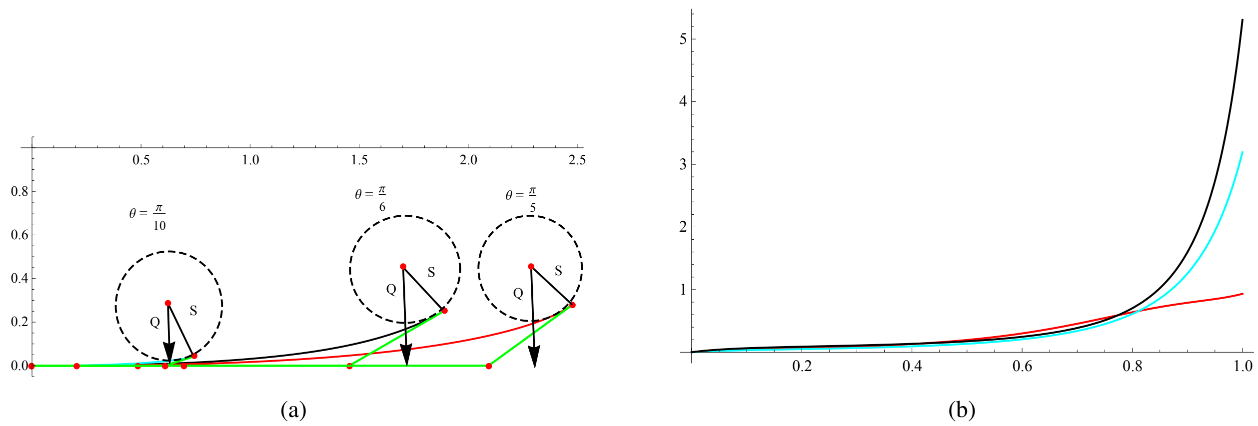

Figure 2. Straight line to circle with cubic GHT-Bézier curve segments and their curvature.

A cubic GHT-Bézier spiral curve gives us a smooth path when its tangent is continuous and curvature for the curve will be monotone. We have chosen different values of shape parameters and θ to obtain a smooth shortest path and curvature for each case is monotone. When we consider $\theta = \frac{\pi}{5}$ and shape parameters $\alpha = -1, \beta = -0.5, \gamma = -1$, then we have concluded from curvature shown in

Figure 2(b) (red curve) that the smooth shortest path will be obtained to reach from an initial location to the final position than the rest one curvature profiles.

4.2. Circle in circle with cubic GHT-Bézier spiral curve

The circle in circle cubic GHT-Bézier spiral curves are defined by using control points as given Eq (4.6).
Position: Consider any two cubic GHT-Bézier spiral curves such that their circle having radius r_0 and r_1 and distance between the radius of two circles is denoted by d. Both the circles lies in first quadrant.
Condition: The solution can be obtained by changing the values of shape parameters $\alpha, \beta, \gamma \in [-1, 1]$ and angle θ.

- In Figure 3(a), the circle in circle cubic GHT-Bézier spiral curves with shape parameters $\alpha = \beta = \gamma = 1$ and $\alpha = 0.5, \beta = 0.5, \gamma = 0$ respectively are shown. Here, the solution (path from origin to the end point of the circle) of cubic GHT-Bézier spiral curve can be obtained when $r_1 - r_0 > d$.
- Similarly, in Figure 3(b), for the shape parameters $\alpha = \beta = \gamma = 0.7$ and $\alpha = 0.5, \beta = 0.5, \gamma = 0$ the solution (path from origin to the edge of the circle) of cubic GHT-Bézier spiral curve can be obtained when $r_1 - r_0 = d$. For both these cases the curves are geometrically smooth. We cannot find any solution when curves are geometrically improper.

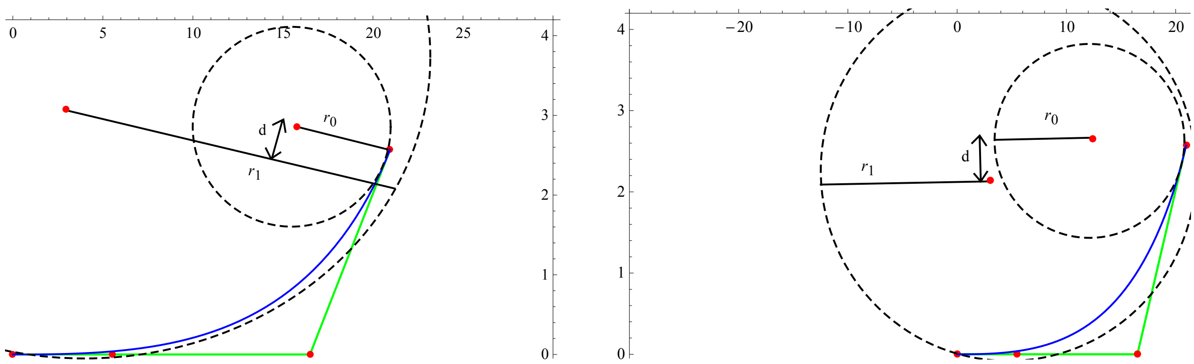

(a) (b)

Figure 3. Circle in circle with cubic GHT-Bézier spiral curve segments.

4.3. Circle to circle forming S-shape curve with two cubic GHT-Bézier spiral curves

Consider any two cubic GHT-Bézier spiral curves $P(u; \alpha, \beta, \gamma) = \sum_{i=0}^{3} \widetilde{P}_i L_{i,3}(u)$ and $Q(u; \hat{\alpha}, \hat{\beta}, \hat{\gamma}) = \sum_{i=0}^{3} \widetilde{Q}_i L_{i,3}(u)$ which are connected to each other and form S-shape curve with spiral curve segments. The control points for first curve segment are $\widetilde{P}_i = (x_i, y_i)$ and for second curve segment the control points are $\widetilde{Q}_i = (-x_i, -y_i)$. So, the control points for an S-shape curve with cubic GHT-Bézier spiral curves can be summarized as follows:

$$\begin{cases} \widetilde{P_1} = \widetilde{P_0} + \frac{50r(1+\frac{\pi}{2}(1+\alpha)-\gamma)tan\theta}{108cos\theta}T_0, \\ \widetilde{P_2} = \widetilde{P_1} + \delta\frac{50r(1+\frac{\pi}{2}(1+\beta)-\gamma)tan\theta}{108cos\theta}T_0, \\ \widetilde{P_3} = \widetilde{P_2} + \frac{\frac{\pi}{2}(1+\alpha)tan\theta}{18}T_1, \\ \widetilde{Q_1} = \widetilde{Q_0} - \frac{50r(1+\frac{\pi}{2}(1+\hat{\alpha})-\hat{\gamma})tan\theta}{108cos\theta}T_0, \\ \widetilde{Q_2} = \widetilde{Q_1} - \delta_1\frac{50r(1+\frac{\pi}{2}(1+\hat{\beta})-\hat{\gamma})tan\theta}{108cos\theta}T_0, \\ \widetilde{Q_3} = \widetilde{Q_2} - \frac{\frac{\pi}{2}(1+\hat{\alpha})tan\theta}{18}T_1. \end{cases} \tag{4.7}$$

Position: The two cubic GHT-Bézier spiral curves are connected at origin (where curvature and tangent both are equally zero) to form an S-shape curve. Let r_0 and r_1 be the radius of two circles (ξ_0 and ξ_1) which lies in the first and third quadrant. Circle ξ_0 lies along the positive y-axis while circle ξ_1 is along the negative y-axis, and d is the distance between the centers of the circles.
Condition: For $\theta = \frac{\pi}{3}$,

- When shape parameters are $\alpha = \beta = \gamma = 0.5$, $\hat{\alpha} = \hat{\beta} = \hat{\gamma} = 0$ then the solution of S-shape curve with two cubic GHT-Bézier spiral curves is obtained when $r_0 + r_1 < d$ where $r_0 = r_1 = 0.75$ and $d = 3.2$ as shown in Figure 4(a).
- If the shape parameters are $\alpha = \beta = \gamma = -0.5$ and $\hat{\alpha} = \hat{\beta} = \hat{\gamma} = 0$, then solution of S-shape curve with two cubic GHT-Bézier spiral curve segments is obtained when $r_0 + r_1 \approx d$ as given in Figure 4(b). The parameter values for $r_0 = r_1 = 1$ and $d = 2.2$.
- The S-shape curve by cubic GHT-Bézier spiral curve segments are geometrically improper when $r_0 + r_1 > d$, and in this case no solution about smoothness of curve can be found.

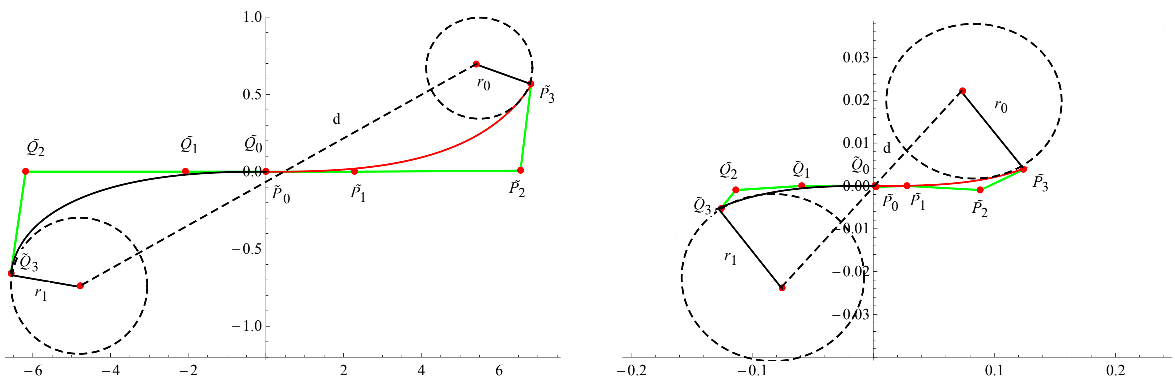

(a) (b)

Figure 4. S-shape curve with cubic GHT-Bézier spiral curve segments.

4.4. Circle to circle forming C-shape curve with two cubic GHT-Bézier spiral curves

Consider any two cubic GHT-Bézier spiral curves $P(u;\alpha,\beta,\gamma) = \sum_{i=0}^{3}\widetilde{P}_iL_{i,3}(u)$ and $Q(u;\hat{\alpha},\hat{\beta},\hat{\gamma}) = \sum_{i=0}^{3}\widetilde{Q}_iL_{i,3}(u)$, and a C-shape curve is composed by joining these two cubic GHT-Bézier spiral curve segments. The control points for constructing C-shape curve can be summarized in the following equation:

$$
\begin{cases}
\widetilde{P_1} = \widetilde{P_0} + \frac{50r(1+\frac{\pi}{2}(1+\alpha)-\gamma)tan\theta}{108cos\theta}T_0, \\
\widetilde{P_2} = \widetilde{P_1} + \delta\frac{50r(1+\frac{\pi}{2}(1+\beta)-\gamma)tan\theta}{108cos\theta}T_0, \\
\widetilde{P_3} = \widetilde{P_2} + \frac{\frac{\pi}{2}(1+\alpha)tan\theta}{18}T_1, \\
\widetilde{Q_1} = \widetilde{Q_0} - \frac{50r(1+\frac{\pi}{2}(1+\hat{\alpha})-\hat{\gamma})tan\theta}{108cos\theta}T_0, \\
\widetilde{Q_2} = \widetilde{Q_1} - \delta_1\frac{50r(1+\frac{\pi}{2}(1+\hat{\beta})-\hat{\gamma})tan\theta}{108cos\theta}T_0, \\
\widetilde{Q_3} = \widetilde{Q_2} + \frac{\frac{\pi}{2}(1+\hat{\alpha})tan\theta}{18}T_1.
\end{cases}
\tag{4.8}
$$

Position: The two circles ξ_0 and ξ_1 have radius r_0 and r_1 lies in first and second quadrant. So, the control points for first cubic GHT-Bézier spiral curve segment are $\widetilde{P_i} = (x_i, y_i)$ and for second cubic GHT-Bézier spiral curve segment the control points are as $\widetilde{Q_i} = (-x_i, y_i)$.
Condition:

- For $\theta = \frac{\pi}{4}$, and for the shape parameters $\alpha = \beta = 0.5, \gamma = 0$, and $\hat{\alpha} = \hat{\beta} = \hat{\gamma} = 0$ the solution of C-shape curve with cubic GHT-Bézier spiral curve (Ω_1) is obtained when $r_0 + r_1 < D_1$ as shown in Figure 5, where D_1 is the distance between the centers of the circles.
- For $\theta = \frac{\pi}{5}$, and for shape parameters $\alpha = \beta = \gamma = \hat{\alpha} = \hat{\beta} = \hat{\gamma} = 0.5$, the solution of C-shape curve with cubic GHT-Bézier spiral curve (Ω_2) is obtained when $r_0 + r_1 = D_2$ as in Figure 5.

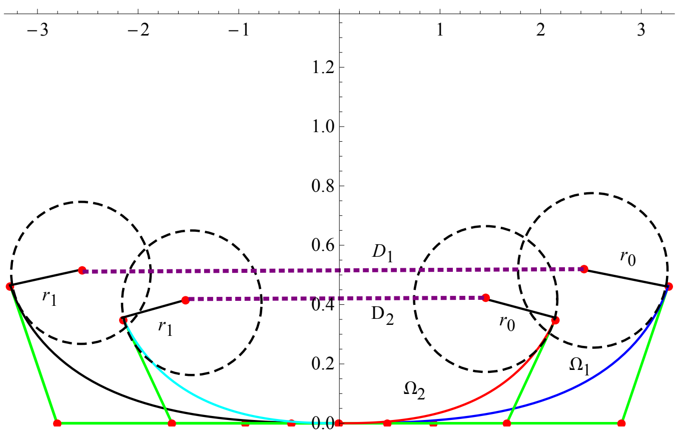

Figure 5. C-shape curve with cubic GHT-Bézier spiral curve segments.

4.5. Line to line with cubic GHT-Bézier spiral curve

Next, line to line of a cubic GHT-Bézier spiral curve are connected to each other and satisfies G^2 continuity. Here two segments of the spiral curve are connected to each other at the joint and their curvature continuity also preserve.

Theorem 3. *The cubic GHT-Bézier spiral curves are connected to each other and satisfy smooth G^2 continuity conditions and have common curvature at the final point of the first curve and initial point of the second curve respectively.*

Proof. Let we have any two cubic GHT-Bézier curves

$$S_1(u;\alpha,\beta,\gamma) = \sum_{i=0}^{3} \widetilde{P}_i L_{i,3}(u), \qquad S_2(u;\hat{\alpha},\hat{\beta},\hat{\gamma}) = \sum_{i=0}^{3} \widetilde{Q}_i L_{i,3}(u)$$

where

$$\kappa_1(u) = \frac{S_1'(u) \times S_1''(u)}{\|S_1'(u)\|^3}, \qquad \kappa_2(u) = \frac{S_2'(u) \times S_2''(u)}{\|S_2'(u)\|^3}$$

and satisfy the following condition,

$$\kappa_1(1) = \kappa_2(0).$$

The control points for line to line GHT-Bézier spiral curves by G^2 continuity are given as follows,

$$\begin{cases} \widetilde{P_1} = \widetilde{P_0} + \frac{50r(1+\frac{\pi}{2}(1+\alpha)-\gamma)tan\theta}{108cos\theta} T_0, \\ \widetilde{P_2} = \widetilde{P_1} + \delta\frac{50r(1+\frac{\pi}{2}(1+\beta)-\gamma)tan\theta}{108cos\theta} T_0, \\ \widetilde{P_3} = \widetilde{P_2} + \frac{\frac{\pi}{2}(1+\alpha)tan\theta}{18} T_1, \\ \widetilde{Q_0} = \widetilde{P_3}, \\ \widetilde{Q_1} = \widetilde{Q_0} + \frac{\frac{\pi}{2}(1+\hat{\alpha})tan\theta}{18} T_1, \\ \widetilde{Q_2} = \widetilde{Q_1} + \delta\frac{50r(1+\frac{\pi}{2}(1+\hat{\beta})-\hat{\gamma})tan\theta}{108cos\theta} T_0, \\ \widetilde{Q_3} = \widetilde{Q_2} + \frac{50r(1+\frac{\pi}{2}(1+\hat{\beta})-\hat{\gamma})tan\theta}{108cos\theta} T_0. \end{cases} \tag{4.9}$$

The graphical representation of line to line cubic GHT-Bézier spiral curve satisfying smooth G^2 continuity conditions is shown in Figure 6. □

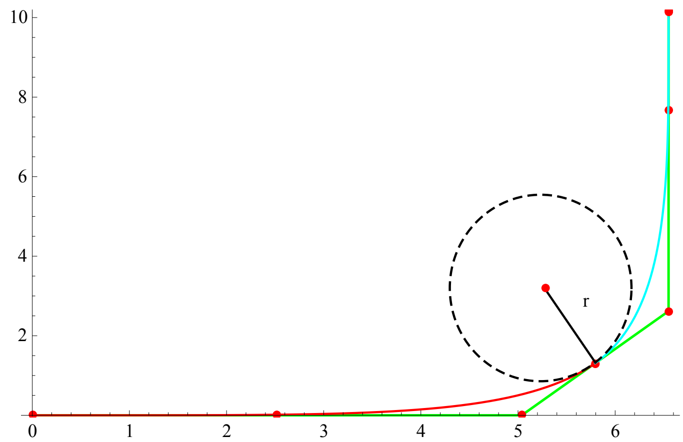

Figure 6. Line to Line cubic GHT-Bézier spiral curve.

For smooth solution, consider any two line segments ℓ_1 and ℓ_2. Here, symmetric line to line transition is shown in Figure 7 and the length for ℓ_1 and ℓ_2 is same.

Position: The line segment ℓ_1 is along the positive y-axis and line segment ℓ_2 is parallel to the x-axis as mentioned in Figure 7.

Condition: At different values of shape parameters $\alpha, \beta, \gamma \in [-1, 1]$ and angle θ, we can obtain multiple solutions. The symmetric representation of line to line cubic GHT-Bézier curve has an extra flexibility in providing the smoothness.

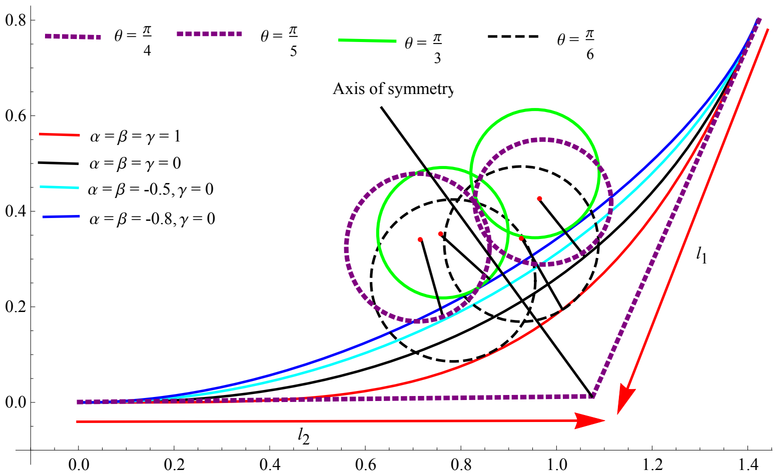

Figure 7. Line to Line with cubic GHT-Bézier spiral curve with $\ell_1 = \ell_2$.

5. Algorithm for proposed smooth path

In this section, an algorithm is presented which provides us a smooth path (free from obstacles) via cubic GHT-Bézier curves. Consider a polyline path having few obstacles. This polyline path can be acquired by any path planning strategy such as visibility graph theory or medial axis theory. Here cubic GHT-Bézier curve provides us many feasible paths, but our required path can be chosen based on Shortest Distance, Bending Energy and Curvature Variation Energy which can be found as follows.

$$\begin{cases} L = Shortest\ \ Distance: & \int_0^1 |S'(u)|du, \\ E = Minimum\ \ Energy: & \kappa(u) = \frac{S'(u)\times S''(u)}{||S'(u)||^3}, \\ V = Curvature\ \ Variation\ \ Energy: & \kappa'(u) = \frac{||S'(u)||^2 \frac{d}{du}(S'(u)\times S''(u)) - 3(S'(u)\times S''(u))(S'(u).S''(u))}{||S'(u)||^5}. \end{cases} \tag{5.1}$$

Since cubic GHT-Bézier curve has three different shape parameters and by adjusting the values of shape parameters we can obtain curvature continuous collision-free path satisfying the above values. The proposed method is generally divided into the following three steps.

1. The shape of the polyline path is partitioned into C-shape sections.
2. Identify the values of variable u which satisfy Farin's G^2 continuity conditions as in [9].
3. Choose the values of shape parameters by which we can obtain an obstacle avoiding the shortest smooth path.

6. Description of smooth path algorithm

In this section, we will describe each step for obtaining a smooth path.

1. **Identification of standard C-shape poly line path**

   A polyline joining the vertices $\widetilde{P_0}, \widetilde{P_1}, ..., \widetilde{P_n}$, is said to be C-shaped as in [9], if the following cross product is either positive or negative. i.e.

$$(\widetilde{P_i} - \widetilde{P_{i-1}}) \times (\widetilde{P_{i+1}} - \widetilde{P_i}), \qquad i = 1, 2, ..., n-1. \tag{6.1}$$

   This C-shaped polyline is in standard form if the cross product given in above Eq (6.1) is positive. Any given C-shape polyline can be reflected across any axis, if necessary, to put it into standard form. So, here we assumed the C-shape in standard form joining the vertices $\widetilde{P_0}, \widetilde{P_1}, \widetilde{P_2}, \widetilde{P_3}$, and it is said to be self-intersecting if it satisfying the following conditions,

$$(\widetilde{P_0} - \widetilde{P_1}) \times (\widetilde{P_3} - \widetilde{P_1}) \geq 0$$

   and

$$(\widetilde{P_0} - \widetilde{P_2}) \times (\widetilde{P_3} - \widetilde{P_2}) \geq 0.$$

   Once the shape is identified, we partitioned the polyline into C-shape sections. Suppose any two cubic GHT-Bézier curves with continuous tangent joined to each other and form a curve. If we choose an inflection point at the mid point of the central vertical lines. Then this inflection point becomes a new vertex in the guiding poly line and form C-shape sections of original curve as shown in Figure 8.

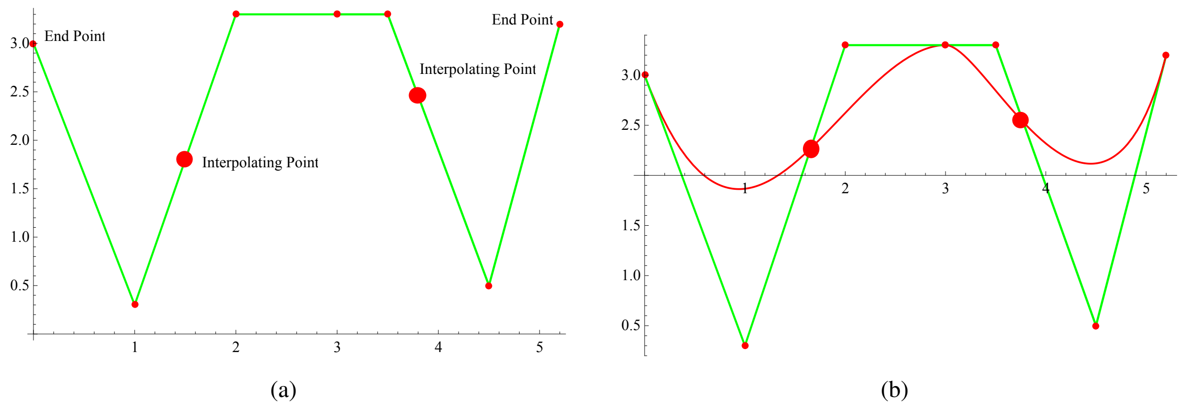

Figure 8. Partitioning of polyline into C-shaped sections.

2. **Identification of variable values which satisfy G^2 continuity conditions**

   After the partitioning into C-shape sections, we treat each C-shape section separately. So, for each C-shape section we can choose values of variable as in Farin's G^2 continuity [9] to ensures that there is no obstacle inside the convex hull of cubic GHT-Bézier curve as in Figure 7(b). By using the chosen variable values and control points of GHT-Bézier spiral curves as in Section 4 and also by varying the values of shape parameters, we can find the Shortest Distance **L**, Bending Energy **E** and Curvature Variation Energy **V** defined in Eq (5.1).

3. **Obtaining the shortest smooth path by different shape parameters**

As we noted that GHT-Bézier curve possesses three different shape parameters $\alpha, \beta, \gamma \in [-1, 1]$, and by adjusting these values of shape parameters we can obtain curvature continuous solutions and smooth shortest path free from obstacles. So, we modify the values of shape parameters until the shortest path is obtained for different cubic GHT-Bézier spiral curve.

7. Numerical examples

In this section, few numerical examples are presented by the implementation of the proposed path smoothing technique using Wolfram Mathematica Software. In Table 4, the comparison between the proposed smooth path algorithm and three more conventional methods [8] for the smooth path as classical Bézier curve, Clothoid and by Log-Aesthetic curve is given.

By using the control points of spiral curves and by varying different values of shape parameters we found the Shortest Distance **L**, Bending Energy **E** and Curvature Variation Energy **V**. From our proposed method, we conclude that cubic GHT-Bézier spiral curve provides us more collision-free smooth path based on Shortest Distance, Bending Energy, and Curvature Variation Energy, as compared to previous methods.

Hence the values of arc length (the shortest path), Bending Energy, and Curvature Variation Energy given in Eq (5.1) can be obtained from the following numerical examples.

Example 7.1. *In this example, we have considered the control points of straight line to circle (or circle to circle) with cubic GHT-Bézier spiral curve as given in Section 4 Eq (4.1). By using these control points we can obtain various solutions of **L**, **E** and **V** (defined in Eq (5.1)) as we change the values of shape parameters and also consider a variable value* 0.6 *which satisfy Farin's* G^2 *continuity conditions [9]. The numerical values of the shortest path **L**, Bending Energy **E** and Curvature Variation Energy **V** are given in Table 1. From this table we can conclude that* 0.75230, 0.0148292 *and* 0.310681 *is smoother shortest value of **L**, **E** and **V** as compared to the path described by previous conventional methods [8].*

Example 7.2. *By having the control points of Eq (4.7), for circle in circle forming S-shape curve with cubic GHT-Bézier spiral curve and also by varying the shape parameters, and a variable value* 0.6 *which satisfy* G^2 *continuity as in [9], we can obtain multiple solutions of **L**, **E** and **V** given in Eq (5.1). The desired values for Shortest path, Bending Energy and Curvature Variation Energy is* 1.13690, 0.002409 *and* 0.019212 *respectively, when we choose* $(\alpha, \beta, \gamma) = (0, -1, 0)$ *given in Table 2. We can deduce from these values that a very convenient shortest smoother value of **L**, **E** and **V** is obtained, as compared to the values by Classical Bézier curve, Clothoid and LACs given in [8].*

Example 7.3. *By similar above discussion, the suitable values of **L**, **E** and **V** between a C-shape curve can also be obtained when we have control points as in Eq (4.8) of the circle to circle forming C-shape curve by cubic GHT-Bézier spiral curve in Eq (5.1). By changing different values of shape parameters we can obtain multiple solutions. From the Table 3, we conclude that when we consider* $(\alpha, \beta, \gamma) = (0, -1, 0)$, *and a variable value* 0.6 *which satisfy* G^2 *continuity as in [9], the Shortest path, Bending Energy and Curvature Variation Energy is obtained.*

Remark 7.1. *In above Examples 7.1–7.3, we have used three templates of spiral curves (Straight line to Circle with cubic GHT-Bézier Spiral curve, Circle to Circle forming S-shape curve with cubic GHT-Bézier Spiral curve, Circle to Circle forming C-shape curve with cubic GHT-Bézier Spiral curve) to* *find Shortest Distance **L**, Bending Energy **E** and Curvature Variation Energy **V**. We can also conclude from Tables 1–3 that by different values of shape parameters α, β, γ for each curve, various solutions can be found. So, we can choose the optimal solution for each curve which is the minimum value of **L**, **E** and **V**. These optimal values are also given in Table 4.*

Table 1. Values of L, E and V from straight line to circle by different values of shape parameters.

Shape parameters (α, β, γ)	Curve Obtained	**L**	**E**	**V**
$(-1, -1, -1)$	Straight line	0.530468	0	0
$(-1, 0, 0)$	Straight line	0.54015	0	0
$(-0.5, 0, 0)$	Circular arc	**0.75230**	**0.0148292**	**0.310681**
$(0, 0, 0)$	Circular arc	0.93687	0.0550361	0.975269
$(0.5, 0, 0)$	Circular arc	1.12903	0.12328	1.67666
$(1, 0, 0)$	Circular arc	1.32873	0.234846	2.02227
$(0, -1, 0)$	Circular arc	0.68450	0.438431	3.07923
$(0, -0.5, 0)$	Circular arc	0.82227	0.148189	1.95236
$(0, 0.5, 0)$	Circular arc	1.02817	0.023941	0.497568
$(0, 1, 0)$	Circular arc	1.09610	0.0182869	0.357975
$(0, 0, -1)$	Circular arc	1.27805	0.0308557	0.855745
$(0, 0, -0.5)$	Circular arc	1.10769	0.0414914	0.975957
$(0, 0, 0.5)$	Circular arc	0.766799	0.0697094	0.709603
$(0, 0, 1)$	Circular arc	0.899880	0.0751205	0.50965

Table 2. Values of L, E and V from circle to circle forming S-shape curve by different values of shape parameters.

Shape parameters (α, β, γ)	Curve Obtained	**L**	**E**	**V**
$(-1, -1, -1)$	Straight line	1.224174	0	0
$(-1, 0, 0)$	Straight line	1.115568	0	0
$(-0.5, 0, 0)$	Circular arc	1.50461	0.007414	0.155339
$(0, 0, 0)$	Circular arc	1.87374	0.0220968	0.391567
$(0.5, 0, 0)$	Circular arc	2.25806	0.0410721	0.558601
$(1, 0, 0)$	Circular arc	2.65746	0.0664824	0.572485
$(0, -1, 0)$	Circular arc	**1.13690**	**0.002409**	**0.019212**
$(0, -0.5, 0)$	Circular arc	1.64454	0.067789	0.893112
$(0, 0.5, 0)$	Circular arc	2.05634	0.008758	0.182032
$(0, 1, 0)$	Circular arc	2.19220	0.004216	0.088529
$(0, 0, -1)$	Circular arc	2.5561	0.009081	0.251859
$(0, 0, -0.5)$	Circular arc	2.21538	0.014089	0.331416
$(0, 0, 0.5)$	Circular arc	1.53359	0.034195	0.348094
$(0, 0, 1)$	Circular arc	2.26068	0.024998	0.050237

Table 3. Values of L, E and V from circle in circle forming C-shape curve by different values of shape parameters.

Shape parameters (α,β,γ)	Curve Obtained	**L**	**E**	**V**
$(-1,-1,-1)$	Straight line	1.22428	0	0
$(-1,0,0)$	Straight line	1.12568	0	0
$(-0.5,0,0)$	Circular arc	1.51461	0.008414	0.165339
$(0,0,0)$	Circular arc	1.88374	0.0221968	0.392567
$(0.5,0,0)$	Circular arc	2.28806	0.0420721	0.568601
$(1,0,0)$	Circular arc	2.66746	0.0674824	0.574485
$(0,-1,0)$	Circular arc	**1.14790**	**0.004409**	**0.029412**
$(0,-0.5,0)$	Circular arc	1.64844	0.068789	0.898312
$(0,0.5,0)$	Circular arc	2.08634	0.009758	0.183032
$(0,1,0)$	Circular arc	2.19420	0.008216	0.089529
$(0,0,-1)$	Circular arc	2.5661	0.009481	0.253859
$(0,0,-0.5)$	Circular arc	2.21638	0.014489	0.335416
$(0,0,0.5)$	Circular arc	1.53369	0.034395	0.349094
$(0,0,1)$	Circular arc	2.26078	0.034998	0.051237

Table 4. Comparison between the values of Shortest Distance, Bending Energy and Curvature Variation Energy.

Curves	**L**	**E**	**V**
Straight line to circle with cubic GHT-Bézier spiral curve	0.75230	0.0148292	0.310681
Circle in Circle forming S-shape with cubic GHT-Bézier spiral curve	1.13690	0.002409	0.019312
Circle in Circle forming C-shape with cubic GHT-Bézier spiral curve	1.14790	0.004409	0.029412
Classical Bézier curve [8]	3.31	0.255	30.96
Clothoid [8]	3.324	0.383	4.60
Log-Aesthetic curve [8]	3.30	0.175	7.28

From Table 4, it is clear that the obstacle avoiding smooth path which is obtained by the proposed method is convenient to move from any initial location to the final position. The values for minimization of the **L**, **E** and **V** are obvious in Table 4. Hence, we conclude that our proposed method provides a flexible Shortest smooth path, Bending Energy and Curvature Variation Energy as compared to the methods described previously.

8. Conclusions

In this paper, five templates of spiral transition curves by using cubic GHT-Bézier curve are described. An algorithm is presented which provides us a smooth path (free from obstacles) via cubic GHT-Bézier spiral curves. We obtained a smooth (obstacle-free) path by minimization of the Shortest Distance, Bending Energy, and Curvature Variation Energy. By varying different values of shape parameters we obtained multiple solutions where the desired value is considered by the minimum (arc length) **L**, **E** and **V**. Some numerical examples are also presented which demonstrate the flexibility of smooth path and ensures that this technique (algorithm for a smooth path by the cubic GHT-Bézier spiral curve) is more flexible in providing smooth obstacle avoiding path as compared to the previous conventional methods described in [8]. The comparison between the proposed method and methods described earlier is given in Table 4. Moreover, we may extend the current algorithm by identifying the variable values which satisfy G^3 continuity. In this way, a more smooth obstacle-avoiding path can be easily obtained.

Acknowledgments

This research is supported by the Ministry of Higher Education Malaysia through Fundamental Research Grant Scheme (FRGS/1/2020/STG06/USM/03/1) and School of Mathematical Sciences, Universiti Sains Malaysia.

Conflict of interest

The authors declare that they have no conflict of interests regarding the publication of this paper.

References

1. G. Farin, *Curves and Surfaces for CAGD*, San Diego: Academic Press, 2002.
2. D. J. Walton, D. S. Meek, A planar cubic Bézier spiral, *J. Comput. Appl. Math.*, **72** (1996), 85–100.
3. M. Y. Misro, A. Ramli, J. M. Ali, N. N. A. Hamid, Cubic trigonometric Bézier spiral curves, *2017 14th International Conference on Computer Graphics, Imaging and Visualization*, (2017), 14–20.
4. D. J. Walton, D. S. Meek, G^2 curve design with a pair of Pythagorean hodograph quintic spiral segments, *Comput. Aided Geom. Des.*, **24** (2007), 267–281.
5. M. Y. Misro, A. Ramli, J. M. Ali, N. N. A. Hamid, Pythagorean hodograph quintic trigonometric Bézier transition curve, *2017 14th International Conference on Computer Graphics, Imaging and Visualization*, (2017), 1–7.
6. Z. Habib, M. Sakai, G^2 cubic transition between two circles with shape control, *J. Comput. Appl. Math.*, **223** (2009), 133–144.
7. M. Y. Misro, A. Ramli, J. M. Ali, S-shaped and C-shaped transition curve using cubic trigonometric Bézier, *AIP Conf. Proc.*, **1870** (2017), 050005.
8. R. U. Gobithaasan, S. W. Yip, K. T. Miura, M. Shanmugavel, Optimal path smoothing with log-aesthetic curves based on shortest distance, minimum bending energy and curvature variation energy, *Proc. CAD'19*, (2019), 397–402.
9. Z. Li, D. S. Meek, D. J. Walton, A smooth, obstacle-avoiding curve, *Comput. Graphics*, **30** (2006), 581–587.
10. M. Y. Misro, A. Ramli, J. M. Ali, Extended analysis of dynamic parameters on cubic trigonometric Bézier transition curves, *2019 23rd International Conference in Information Visualization–Part II*, (2019), 141–146.

11. M. Y. Misro, A. Ramli, J. M. Ali, Construction of quintic trigonometric Bézier spiral curve, *ASM Sci. J.*, **12** (2019), 208–215.

12. T. Mauga, New spiral curves for appropriate transition of minimum roadside clearance on simple curves, *J. Transp. Technol.*, **5** (2015), 141–158.

13. K. G. Baass, The use of clothoid templates in highway design, *Transportation Forum*, (1984), 47–52.

14. S. Havemann, J. Edelsbrunner, P. Wagner, D. W. Fellner, Curvature controlled curve editing using piecewise clothoid curves, *Comput. Graphics*, **37** (2013), 764–773.

15. K. T. Miura, D. Shibuya, R. U. Gobithaasan, S. Usuki, Designing log-aesthetic splines with G^2 continuity, *Comput.-Aided Des. Appl.*, **10** (2013), 1021–1032.

16. R. U. Gobithaasan, S. W. Yip, K. T. Miura, Log-aesthetic curves for shape completion problem, *J. Appl. Math.*, **2014** (2014), 960302.

17. S. BiBi, M. Abbas, K. T. Miura, M. Y. Misro, Geometric modelling of novel generalized hybrid trigonometric Bézier-like curve with shape parameters and its applications, *Mathematics*, **8** (2020), 967.

18. S. BiBi, M. Abbas, M. Y. Misro, G. Hu, A novel approach of hybrid trigonometric Bézier curve to the modeling of symmetric revolutionary curves and symmetric rotation surfaces, *IEEE Access*, **7** (2019), 165779–165792.

19. G. Hu, J. L. Wu, X. Q. Qin, A novel extension of the Bézier model and its applications to surface modeling, *Adv. Eng. Software*, **125** (2018), 27–54.

20. G. Hu, C. C. Bo, G. Wei, X. Q. Qin, Shape adjustable generalized Bézier surfaces: Construction and its geometric continuity conditions, *Appl. Math. Comput.*, **378** (2020), 125215.

21. G. Hu, J. L. Wu, Generalized quartic H-Bézier curves: Construction and application to developable surfaces, *Adv. Eng. Software*, **138** (2019), 102723.

22. X. D. Chen, W. Ma, Geometric point interpolation method in space with tangent directional constraint, *Comput.-Aided Des.*, **44** (2012), 1217–1228.

23. M. Ammad, M. Y. Misro, M. Abbas, A. Majeed, Generalized developable cubic trigonometric Bézier surfaces, *Mathematics*, **9** (2021), 283.

24. M. Ammad, M. Y. Misro, Construction of local shape adjustable surfaces using quintic trigonometric Bézier curve, *Symmetry*, **12** (2020), 1205.